Ann. Geophys., 29, 583–590, 2011
www.ann-geophys.net/29/583/2011/
doi:10.5194/angeo-29-583-2011

Annales Geophysicae

Possible interaction between thermal electrons and vibrationally excited N_2 in the lower E-region

K.-I. Oyama[1], M. Shimoyama[2], J. Y. Liu[3], and C. Z. Cheng[1]

[1]Plasma and Space Science Center, National Cheng Kung University, No.1 Ta-Hshue Rd, Tainan, Taiwan
[2]Institute of Space and Astronautical Science, Japan Aerospace Exploration Agency, Sagamihara, Japan
[3]National Central University, Jhongda-Rd, ChungLi, Taiwan

Received: 23 June 2009 – Revised: 13 January 2011 – Accepted: 16 March 2011 – Published: 25 March 2011

Abstract. As one of the tasks to find the energy source(s) of thermal electrons, which elevate(s) electron temperature higher than neutral temperature in the lower ionosphere E-region, energy distribution function of thermal electron was measured with a sounding rocket at the heights of 93–131 km by the applying second harmonic method.

The energy distribution function showed a clear hump at the energy of ∼0.4 eV. In order to find the reason of the hump, we conducted laboratory experiment. We studied difference of the energy distribution functions of electrons in thermal energy range, which were measured with and without EUV radiation to plasma of N_2/Ar and N_2/O_2 gas mixture respectively. For N_2/Ar gas mixture plasma, the hump is not clearly identified in the energy distribution of thermal electrons. On the other hand for N_2/O_2 gas mixture, which contains vibrationally excited N_2, a clear hump is found when irradiated by EUV.

The laboratory experiment seems to suggest that the hump is produced as a result of interaction between vibrationally excited N_2 and thermal electrons, and this interaction is the most probable heating source for the electrons of thermal energy range in the lower E-region. It is also suggested that energy distribution of the electrons in high energy part may not be Maxwellian, and DC probe measures the electrons which are non Maxwellian, and therefore "electron temperature" is calculated higher.

Keywords. Ionosphere (Mid-latitude ionosphere; Plasma temperature and density)

Correspondence to: K.-I. Oyama
(oyama@pssc.ncku.edu.tw)

1 Introduction

Since 1959 to 1967, many scientists (Bogges et al., 1959; Spencer et al., 1962, 1965; Brace et al., 1963, 1969; Smith et al., 1968) reported that the electron temperature (T_e) observed with Langmuir probe (Tonks and Langmuir, 1929) was 2–3 times higher than the neutral gas temperature (T_n) in the ionospheric E-region (Oyama et al., 1980).

On the other hand theory always says that T_e should be equal to T_n in the lower E-region, because neutral density is about 10^{12} particles/cc, and electron density (N_e) during daytime is 10^5 els/cc. Because of this reason some scientists doubted the reliability of Langmuir probe experiment. We know that DC Langmuir probe cannot give reliable measurement when the electrode surface is contaminated (Smith, 1972; Sturges, 1973; Hirao and Oyama, 1973; Oyama, 1976; Amatucci et al., 2001). Almost without exception the surface of the electrode is contaminated. However even we remove the effect of electrode contamination or use the instrument which can avoid the electrode contamination (Hirao and Oyama, 1970; Oyama and Hirao, 1976), T_e measured by DC Langmuir probe is higher than model T_n (Oyama et al., 1980; Duhau and Azpiazu, 1985; Amemiya et al., 1985), although very rarely we observed T_e which is very close to T_n (Hirao and Oyama, 1973; Rohde et al., 1993).

In addition to the above, in the E-region the electron collision frequency evaluated from the radio wave absorption in the E-region is higher than that from scattering cross sectional data and that from model atmosphere (Schlapp, 1959). As the electron collision frequency is nearly proportional to T_e, collision frequency could be explained with the high T_e observed with Langmuir probe. This idea was also presented by Beynon and Owen Jones (1965), and Thrane and Piggot (1966). Moreover Walker (1968) tried to explain the high T_e in the E-region as due to the vibrational temperature (T_v)

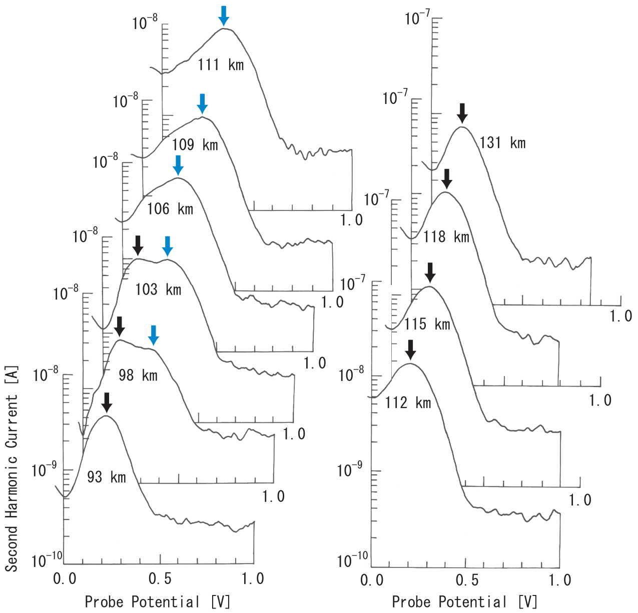

Fig. 1. Second harmonic components at the heights of 93–131 km. Horizontal axis is the probe potential (energy of electrons) and vertical axis is the second harmonic component in amperes. Please note the second peak marked by a blue arrow at the heights of 98 km, 103 km, 106 km, 109 km and 111 km. The symptom of the peak starts to appear from the height of 98 km. The current below 3×10^{-10} A is noise of the amplifier.

of the nitrogen molecules. However later he wrote another paper, mentioning that T_v cannot explain high T_e. Pavlov (1994) discusses the role of vibrationally excited nitrogen molecules in the D- and E-regions of the ionosphere, and concludes that the effect of the vibrationally excited nitrogen gas cannot explain experimentally observed higher T_e. However we cannot still give up the possibility of the heating of electrons in thermal energy range by vibrationally excited nitrogen molecules as we discuss here.

Our recent measurement of T_e around irregular structure of sporadic E-layer (Oyama et al., 2008) shows that T_e in the low density region is higher than the model T_n, and T_e starts reducing toward T_n as the probe moves into the Es layer. The electron energy density ($k \cdot N_e \cdot T_e$; k is Boltzmann constant, and N_e/T_e are measured electron temperature and density) shows the maximum around the height region of 100–120 km. Therefore we suggested that heat source which elevates T_e higher than model T_n should exist at the height of around 100–120 km.

As such, in spite of the effort to solve the problem, gradually the number of the paper reduced as scientists could not explain T_e which is higher than T_n. We cannot still reach a firm conclusion on this apparently simple problem.

Here we present one experimental result, which seems to suggest the important role of vibrationally excited molecular nitrogen gas for the heating of thermal electrons in the lower E-region, We also mention that T_e values which were observed higher than T_n in the past might be due to the non-Maxwellian of electron in thermal energy range.

2 Data obtained in space

Figure 1 shows a set of data on the energy distribution function obtained by a sounding rocket S-310-14, which was launched from Kagoshima Space Center (Geographic latitude/longitude, 31° N/131° E; geomagnetic latitude, 24° N) at 18:16:50 JST (09:16:50 UT) on 16 September 1983. Geomagnetic index Kp and F10.7 solar radio flux are 4^- (09:00–12:00 UT) and 105.1 sfu, respectively. We used a glass-sealed Langmuir probe (Oyama and Hirao, 1976) in order to get the second derivative of DC current voltage ($v-i$) characteristic curves, which is a direct indicator of energy distribution function. According to an equation which provides the relationship between energy distribution function *F(eV)* and the second derivative of the DC current voltage characteristic curve, (d^2i/dV^2) with respect to the electrode potential (Druyvesteyn, 1930) is written as

$$F(eV) = [4m^{1/2}V^{1/2}/2^{1/2}Se^{5/2}](d^2i/dV^2), \tag{1}$$

where S is the probe area, and e and m are charge and mass of electron respectively. V is the probe voltage measured from space plasma potential, which correspond to the energy of electrons.

The second derivative of the curve is obtained by superposing a small sinusoidal signal of frequency f on the probe sweep voltage and by picking up the second harmonic components i_{2f} from the probe current, that consists of DC current and, harmonic components of the fundamental frequency, $2f$ (Boyd and Twiddy, 1959). The relationship between the second harmonic component i_{2f} and the second derivative of $v-i$ curve is expressed by the following equation,

$$i_{2f} \sim -a^2/4 \cdot (d^2i/dV^2) \tag{2}$$

where a is an amplitude of small sinusoidal signal. If the electrons in plasma are Maxwellian, DC probe electron current is expressed as $i \sim e \cdot S \cdot N_e \cdot (kT_e/2m)^{1/2} \cdot \exp(-eV/kT_e)$ in the electron retardation regime, and the semi-logarithmically plotted i produces a liner relationship between probe voltage and probe electron current. The second derivative of the $v-i$ curve also gives the exponential function, and therefore semi-logarithmically plotted second harmonic component again indicates a linear relation between the probe potential and the semi-logarithmically plotted second harmonic component. Therefore in order to check the Maxwellian distribution, the amplitude of the second harmonic component, that is detected, and is fed to a logarithmic amplifier onboard the rocket. If the output signal from the logarithmic amplifier versus the probe voltage does not show the linear relation in the energy range which we are interested in, the electrons are considered to be non-Maxwellian.

Energy distribution function is therefore expressed as,

$$F(eV) = C(4/a^2)i_{2f}, \tag{3}$$

where $C = -4m^{1/2}V^{1/2}/(2^{1/2}Se^{5/2})$.

Energy distribution function of electrons in thermal energy range has been so far measured by using the technique, that is described above, in Japan (Oyama and Hirao, 1979, 1983, 1985). Figure 1 shows the semi-logarithmically plotted second harmonic components, which were obtained from the height of 93 km to 111 km (left), and from 112 km to 131 km (right), respectively. The horizontal axis shows the probe potential with respect to space plasma potential, which corresponds to the energy of thermal electrons.

In the figure, the second harmonic component shows the minimum around the potential, which should be close to the space potential. The location of the space potential is still controversial whether we should take the minimum of the second harmonic component or the peak (Hirao and Oyama, 1971), which appears at around 0.2 eV at 93 km, 112 km, 115 km, 118 km, and 131 km, which is indicated by a black arrow. Here we defined space potential as the minimum of the second harmonic component. The ideal second harmonic component (second derivative) should extend toward space potential from the peak and should be zero at space potential after the steep reduction. However the actual second harmonic current versus probe voltage shows the rounding of the curve, and is not zero, although it shows the minimum around the space potential. The mechanism of the reduction of current near space potential is not clear. One idea, which has been proposed, is that near space potential very low energy of thermal electrons are repelled from the electrode. Another is that work function of the electrode is different over each part of the surface, and final $v-i$ curve is a summation of $v-i$ curves from these small areas. The second harmonic current signal shown in Fig. 1 is buried in the amplifier noise below the current of 3×10^{-10} A for this experiment.

What we would like to stress here are two. One is a peak, which starts to appear at the energy of 0.4 eV at 98 km, marked by a blue arrow. The peak becomes comparable to the first peak marked by black arrow at the height of 103 km. In this case, the first peak is not a real peak as we mentioned above. At the height of 106 km, 109 km, and 111 km, only the second peak can be seen. At the height of 112 km, the peak position suddenly comes back to 0.2 eV and keeps nearly the same value.

Another point which should be mentioned is that the semi-logarithmically plotted second harmonic component, corresponding to the second derivative of the DC probe curve, is not linear especially at the heights of 98 km and 103 km, although at other heights as well the curve is not purely linear. This suggests that thermal electrons are not Maxwellian for this experiments (Oyama and Hirao, 1979).

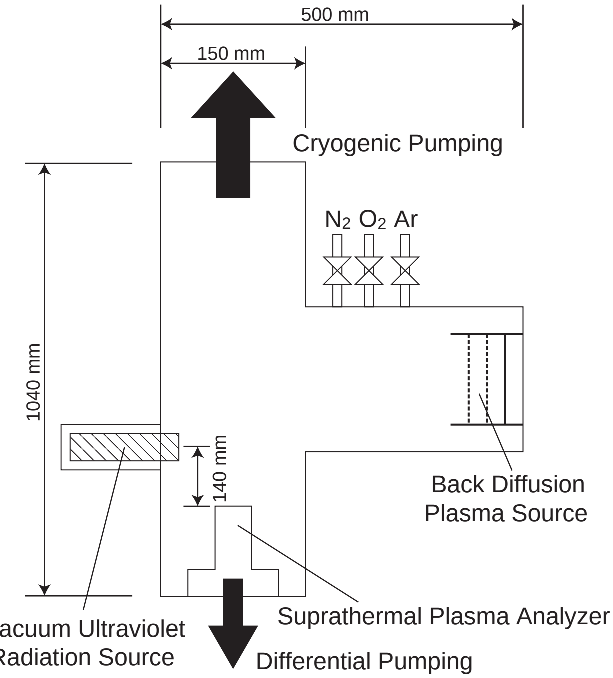

Fig. 2. Experimental set up to measure second harmonic component which provides energy distribution of electrons in thermal energy range. The test chamber is evacuated using a cryo-genic pump. The sensor part is pumped by another turbo-molecular pump. Back diffusion type plasma source produces plasma which is similar to ionospheric plasma, although T_e in the laboratory plasma is much higher than that around 100 km.

Until recently we could not find any physical explanation on these peculiar features in spite of the firm confidence that the measurement is reliable. We recently conducted a laboratory experiment to find the reason for the second peak. The experiment suggests that this peak appears as the result of interaction between vibrationally excited molecular nitrogen and electrons in thermal energy range as we describe in the next section.

3 Laboratory experiments on the role of N_2

Two kinds of experiment were conducted to study the role of vibrationally excited N_2. One is to excite molecular nitrogen vibrationally, and secondly to heat thermal electrons through vibrationally excited N_2. It is noted that N_2 gas which is vibrationally excited by suprathermal electrons, heats the electrons in thermal energy range.

Experimental set-up is shown in Fig. 2. 1040 mm in length and 150 mm in diameter. The test space is evacuated by a cryo-genic pump. We injected N_2, Ar gas individually, mixture of N_2/Ar and mixture of N_2/O_2. We changed the pressure of each gas, while keeping total pressure inside the test chamber at the pressure of 10^{-1} Pa (7.6×10^{-4} Torr). The pressure

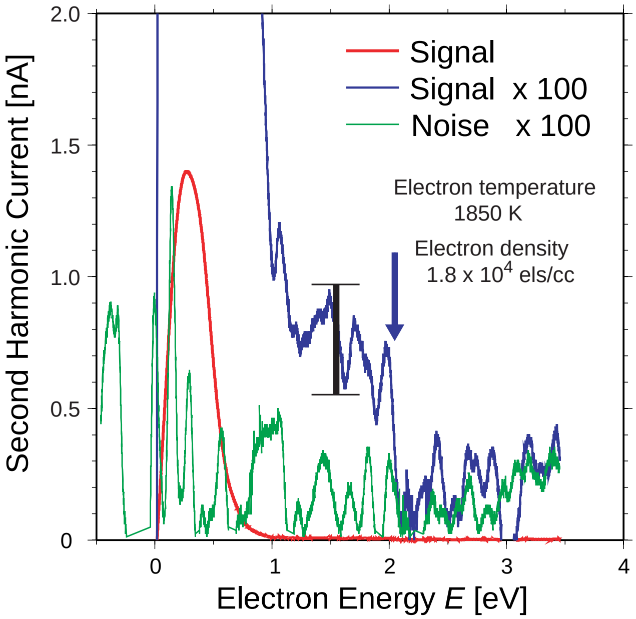

Fig. 3. The second harmonic component. Amplitude of sinusoidal wave superposed to the probe sweep voltage is 200 mV. The second harmonic components discriminated by blue line is amplified 100 times higher than the red curve. The green line shows noise when the second harmonic component marked by red line is amplified 100 times. N_2 gas pressure and N_e are 1×10^{-1} Pa, and 1.8×10^{4} els/cc, respectively. T_e that is calculated from thermal energy is 1850 K. Please note that the signal drops sharply around 2 eV. The black vertical line indicated the magnitude of the noise. A blue arrow indicates the energy where the second harmonic component reduces drastically.

of 10^{-1} Pa (7.6×10^{-4} Torr) is one order higher than the pressure at the height of ∼100 km. The injected gas is ionized by a back diffusion type of plasma source. The plasma density produced is in the order of 10^5 els/cc, which is very close to the day time plasma density at the height of ∼100 km.

The second harmonic current (which is needed to get energy distribution) of electrons in thermal or non-thermal range was measured by a newly developed instrument. The measurement principle is based on the second harmonic method, which has been used for the rocket experiment. We combined a Retarding Potential Analyzer and the second harmonic method. The first circular electrode of a sensor has an entrance hole of 1 mm in diameter at the center for electrons. The hole is masked by the mesh of 500 mesh/inch. The mesh thickness is 0.01 mm. A sweep voltage (0–5 V) which is modulated by a sinusoidal wave of 2 kHz in frequency and 200 mV in amplitude is applied to the first electrode. At the back of the first electrode, an electron multiplier is placed to pick up electrons. The entrance of the electron multiplier is biased to +200 V to attract electrons. The sensor part was evacuated below the pressure of 10^{-3} Pa (7.6×10^{-6} Torr) by a small turbo-molecular pump, so that electron multiplier which needs high voltage can work. The electron multiplier is used as a current mode. 4 kHz sinusoidal component is selected from the multiplier current by a filter, which corresponds to the second derivative of the voltage-electron current characteristic curve (Shimoyama et al., 2011).

The main reaction to produce of $O(^1D)$ around 100 km is (Torr and Torr, 1982)

$$O_2 + h\nu\ (135\text{-}175\,\text{nm}) \rightarrow O(^3P) + O(^1D). \tag{4}$$

Therefore in order to produce $O(^1D)$, EUV whose wave length is longer than 100 nm was radiated by a Deuteron Lamp, through magnesium-fluoride window (Oyama et al., 1991). The radius of the window is 10 mm. The light intensity of the EUV lamp is $1.9\times10^{-5}\,\text{W cm}^{-2}$ (about 20 times solar intensity) at 121.6 nm, $2.0\times10^{-7}\,\text{W cm}^{-2}$ (about 68 times of solar intensity) at 128 nm, and 0.75 times the solar light for 210–250 nm at 5 cm from UV lamp window. When the distant is 10 cm apart from the window, the intensities for these wavelengths become 1/4.

3.1 Experiment on the vibrational excitation of N_2 by supra-thermal electrons

Figure 3 provides the second harmonic component, that was measured to show the evidence of vibrational excitation of N_2 gas by suprathermal electrons. The suprathermal electrons exist in the plasma, which is produced by a back diffusion type plasma source. Plasma density is 1.8×10^{4} els/cc in the N_2 gas pressure of 10^{-1} Pa (7.6×10^{-4} Torr). T_e is about 1850 K. The magnitude of the noise is indicated by a black vertical bar. Steep reduction of the second harmonic component is marked by a blue arrow. It starts at the energy of about 1.9 eV. At the energy higher than 2.2 eV, the second harmonic component starts to increase gradually. The figure shows that electrons which have the energy of 1.9–3 eV is used to excite N_2 gas vibrationally. The result is qualitatively consistent with the result by Schutz (1964), who showed the large cross section of N_2 for the vibrational excitation by electrons which have higher than 2 eV in the energy range of 2–3 eV. The sum of the vibrational cross sections to individual state starts increasing at around 1.84 eV and takes the maximum at 2 eV. In this energy range the cross section increases from 0.3×10^{-16} to 3×10^{-16} in arbitrary scale. From about 2.2 eV toward 3.5 eV the cross section gradually reduces to zero. The fact that sudden drop of the second harmonic current found in the measurements shown in Fig. 3 is found nearly at the same energy as was mentioned by Shutz seems to support our assumption which we mentioned in Fig. 1, that the space plasma potential (0 energy in the energy distribution function) is at the probe potential where the second harmonic component shows the minimum.

The experiment reported in this paragraph suggests that suprathermal electron excite N_2 vibrationally. However the number density of the vibrationally excited N_2 is not enough to heat thermal electron in this case. In order to see the role

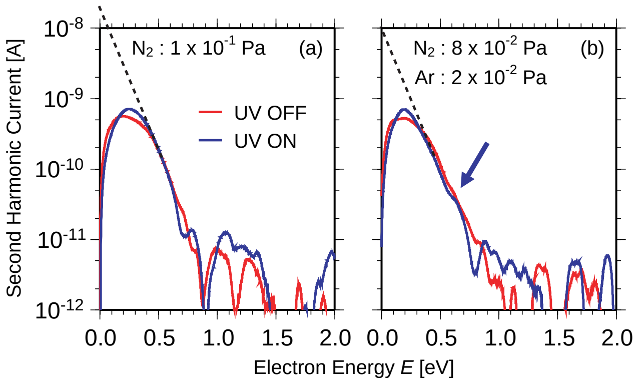

Fig. 4. Second harmonic component of thermal electrons in N_2 gas only **(a)** and mixture of N_2/Ar **(b)** when EUV lamp was turned on (blue line) and off (red line). Pressure inside the test chamber is 1×10^{-1} Pa for pure N_2 gas experiment, and for mixture gas experiment pressure of N_2 and Ar gas were 8×10^{-2} Pa and 2×10^{-2} Pa, respectively. The blue arrow in the right panel indicates the energy where a small hump exists. Two short tip marks between two 10 increment-long tip marks indicate 2, and 5 respectively.

of vibrationally excited N_2 played for the heating of thermal electrons, number density of vibrationally excited N_2 should be increased as we describe below.

3.2 Experiment on the heating of thermal electrons by vibrationally excited nitrogen

Another channel to excite N_2 vibrationally besides suprathermal electrons is a following reaction (Kummler and Bortner, 1972; Harris and Adams, 1983; Slanger and Black, 1974):

$$O(^1D)+N_2 \rightarrow N_2(v)+O(^3P). \tag{5}$$

Vibrationally excited N_2 gas thus generated gives energy to the thermal electrons (Gorse et al., 1985; Paniccia et al., 1986).

To study the interaction between low energy electrons with vibrationally excited N_2, the first measurement was done in ionized N_2 gas only, and later by injecting N_2/Ar mixture gas as shown in Fig. 4a and b, respectively. Pressure inside the test chamber is 10^{-1} Pa (7.6×10^{-4} Torr) for pure N_2 gas experiment. After the plasma is produced, EUV lamp was turned on and off. Figure 4a is provided to show the effect of the secondary electrons, which might be produced on the wall of the chamber, as well as sensor case. The second harmonic component was measured during EUV lamp is switched on and off respectively. The reduction of the second harmonic current near space potential (less than 0.3 eV) is always seen, possibly due to the reflection of thermal electrons of low energy from the electrode, as we mentioned before. Figure 4a shows that the effect of the secondary electrons is not large enough to change the energy distribution of electrons in thermal energy range, although the second harmonic current is not the same between EUV on and off.

Figure 4b is provided to show incapability for Ar gas to heat N_2 vibrationally. Ar and N_2 mixture gas is injected in the test chamber. The pressure of N_2 and Ar gas were 8×10^{-2} Pa (6.1×10^{-4} Torr) and 2×10^{-2} Pa (1.5×10^{-4} Torr), respectively. Therefore the pressure in the chamber is about 1 order higher than at the height of ∼100 km. As Fig. 4b shows, a small hump marked by an arrow is identified around the energy of 0.5–0.7 eV, depending on the on/off of EUV lamp.

Finally important role of $O(^1D)$ to excite N_2 vibrationally is shown in Fig. 5a. It shows the second harmonic components for N_2/O_2 gas mixture with the total pressure of 10^{-1} Pa (7.6×10^{-4} Torr). Total gas pressure is kept constant and the ratio of N_2 and O_2 gas pressure was changed. The measurement in the plasma of N_2 gas only is again conducted as shown in the left top panel with EUV on/off. It is noted that even only for N_2 gas the second harmonic component shows a small hump around the energy of 0.5–0.7 eV as a blue arrow indicates. This might be produced by vibrationally excited N_2 molecules, which are produced by the direct excitation of electrons which have energy higher than 2 eV as we described in the previous paragraph.

Other 3 panels of Fig. 5a show the variation of second harmonic component which are measured at different partial pressure of N_2/O_2 mixture gas to see the effect of $O(^1D)$. The pressure of O_2 is increased from 1×10^{-2} Pa (7.6×10^{-5} Torr) (top panel of the right), 2×10^{-2} Pa (1.5×10^{-4} Torr), and to 3×10^{-2} Pa (2.3×10^{-4} Torr) (bottom panel at the right). Accordingly the pressure of N_2 is reduced from 9×10^{-2} Pa (6.8×10^{-4} Torr), 8×10^{-2} Pa (6.1×10^{-4} Torr), and to 7×10^{-2} Pa (5.3×10^{-4} Torr).

Two features should be mentioned in this experiment. First feature is a peak and a hump which appears in the second harmonic component. When EUV is switched on, a peak appears around 0.6 eV as indicated by a black arrow. The peak enhances as the pressure of O_2 increases, as the upper panel of the right and the bottom panel of the left show respectively. A hump which is marked by a blue arrow appears around the energy of 0.7–0.9 eV in the upper panel of the left column, and this hump is more clearly identified as the upper panel of right, and lower panel of the left show respectively as the partial pressure of O_2 increases. The second feature is that the width of the second harmonic component in terms of energy. That is, electrons in high energy regions enhances as the partial pressure of O_2 increases from 0, 1×10^{-2} Pa (7.6×10^{-5} Torr), and 2×10^{-2} Pa (1.5×10^{-4} Torr). Finally as the bottom panel of the right shows, the hump is not identified, and the peak which is marked by a blue arrow is depressed. The successive change of the shape of the second harmonic component from the top left to the bottom right panels suggests that maximum effect of O_2 appears when the ratio of N_2/O_2 pressure is 4/1. Features which are shown in the Fig. 5a are similar to the second harmonic current, which we showed in Fig. 1 at the heights of 98 km, 103 km and 106 km. In Fig. 5b, energy distribution

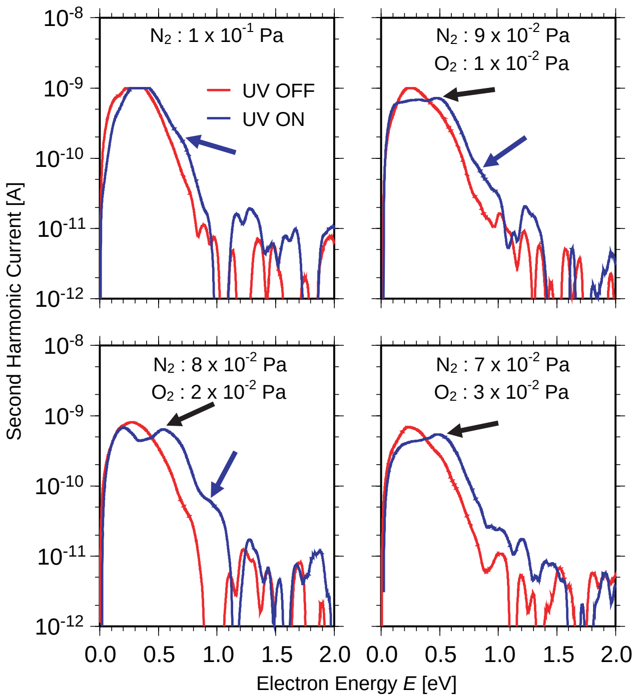

Fig. 5a. Second harmonic components under the N_2/O_2 gas mixture. Right of the top panel shows the case when N_2 and O_2 gas pressure are 9×10^{-2} Pa and 1×10^{-2} Pa, respectively. The left and right panels at the bottom are for the 2×10^{-2} Pa and 3×10^{-2} Pa of O_2, respectively. N_2 pressures are 8×10^{-2} and 7×10^{-2} Pa for each panel so that total pressure inside the test chamber is kept constant at 10^{-1} Pa. Red and blue lines show the second harmonic components without and with radiation of EUV. To compare the shape of the second harmonic component, the second harmonic component of only N_2 gas plasma is shown at the left of the top panel. Black and blue colored arrows indicate the energies where humps appear. Two short tip marks between two 10 increment-long tip marks indicate 2, and 5 respectively.

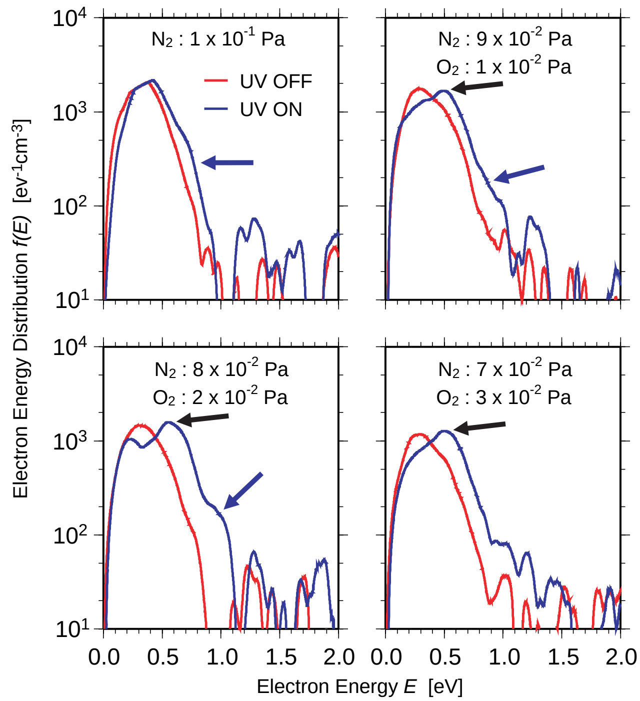

Fig. 5b. The same as for Fig. 5a, but the vertical axis is expressed as electron energy distribution functions, that is calculated according to the Eq. (1).

functions are calculated from Fig. 4a by using Eq. (1). It is noted that the energy gap between first peak which is found around 0.6 eV and the hump which appears at around 0.9 eV is 0.3 eV, which is almost the energy gap of the 1st and 2nd vibrational level of potential curve of N_2.

4 Discussion

The feature of the second harmonic component which was measured by a sounding rocket seems to be reproduced by laboratory experiment as we described above. However we know that laboratory experiment cannot exactly simulate all space conditions, as most of the laboratory experiment has the same fate.

The differences of the second harmonic components between space measurement and laboratory measurement are as followings. First, neutral pressure in laboratory experiment was one order magnitude higher than that at the height of 100 km. Secondary, intensity of solar EUV is different from real situation. This surely causes the discussion on the number of vibrationally excited N_2 produced by $O(^1D)$. Thirdly, T_e in laboratory experiment is more than 5 times higher than at 100 km. In laboratory T_e that we measure by using a back diffusion type of plasma source is 1000–2000 K, and T_e that is measured at the height of ∼100 km is about 200 K on an average. This causes the difference of energy of the second maximum marked by a blue arrow in Figs. 1 and 5. The second harmonic components in space show the second maximum at about 0.4 eV, while laboratory measurements shows the second peak at 0.6 eV.

In spite of these different conditions between laboratory and space, we believe that feature which appeared in the rocket data is caused by vibrationally excited N_2.

In the past, several scientists theoretically discussed the heating of thermal electrons by vibrationally excited N_2 (Gorse et al., 1985; Paniccia et al., 1986). They showed that vibrationally excited nitrogen gas heats low energy electrons in thermal region. Although we did not measure T_v simultaneously, our past laboratory experiment shows that T_v of N_2 is raised to 1000–2000 K in the mixture gas of N_2/O_2 under the irradiation of EUV (Zalpuri and Oyama, 1991).

So far we obtained the energy distribution function, together with T_e, and T_v of N_2 separately (Kurihara and Oyama, 2005) by different sounding rocket. T_e and T_v values show almost the same value, and T_v is very close to the value, which has been calculated by taking into account the role of $O(^1D)$ (Oyama and Hirao, 1985; Kummler and Bortner, 1972).

5 Concluding remarks

We have conducted a laboratory experiment to understand an interesting feature of second harmonic components obtained by a sounding rocket at the height of ∼100 km. The laboratory experiment appears to suggest that vibrationally excited molecular nitrogen is interacting with thermal electrons at the heights of ∼100 km (Oyama and Hirao, 1979). It is also noted that energy distribution is not fully Maxwellian, and electron density in the high energy part is enhanced because of the interaction as we found by sounding rocket experiments (Oyama and Hirao, 1976, 1979, 1983). If this is the case, T_e which is calculated by using DC Langmuir probe gives T_e which is higher than model T_n, because energy range to calculate T_e from Langmuir probe is around the floating potential of $v-i$ characteristic curve, where high energy particles exist.

The energetics at the height of ∼100 km regarding T_e is still not clear even in mid latitude. To study the mystery, which has not been made clear, measurement of energy distribution of electrons in thermal and suprathermal regions is needed, because DC Langmuir probe has a difficulty to provide information on whether high energy tail exists.

Acknowledgements. The authors would like to express their thanks to the launching crew of the Institute of Space and Astronautical Science (ISAS). The authors also should express their sincere gratitude for the cooperation of related government institutions, which made the experiment successful. The laboratory experiment was conducted by using facilities at ISAS with the support of Space Plasma Committee of ISAS. The manuscript was completed while K.-I. Oyama was visiting National Central University, and National Cheng Kung University, Taiwan in 2007–2010.

Topical Editor M. Pinnock thanks P. Muralikrishna and another anonymous referee for their help in evaluating this paper.

References

Amatucci, W. E., Schunk, P. W., Walker, D. N., Kintner, P. N., Powel, S., Holback, B., and Leonhardt, D.: Contamination-free sounding rocket Langmuir probe, Rev. Sci. Instr., 72, 2053–2057, 2001.

Amemiya, H., Oyama, K., and Hirao, K.: Observation of the energy distribution of thermal electrons in the mid latitude ionosphere, Planet. Space Sci., 33, 875–890, 1985.

Beynon, W. J. G. and Owen Jones, E. S.: Seasonal variations in the lower and upper atmosphere, Nature, 206, 1243–1245, 1965.

Bogges, R. L., Brace, L. H., and Spence, N. W.: Langmuir probe measurements in the ionosphere, J. Geophys. Res., 64, 1627–1630, 1959.

Boyd, R. L. F. and Twiddy, N. D.: Electron energy distribution in Plasma 1, Proc. Roy. Soc., A250, 53–69, 1959.

Brace, L. H., Spencer, N. W., and Carignan, G. R.: Ionospheric electron temperature measurements and their implications, J. Geophys. Res., 68, 5397–5412, 1963.

Brace, L. H., Carson, H. C., and Mahajan, K. K.: Radar backscatter and Rocket Probe measurements of electron temperature above Arecibo, J. Geophys. Res., 74, 1883–1885, 1969.

Druyvesteyn, M. J.: Der Niedervoltbogen, Zeits. Phys., 64, 781–798, 1930.

Duhau, S. and Azpiazu, M. C.: Empirical model of the E region electron temperature around noon and at low magnetic activity, Planet. Space. Sci., 33, 909–914, 1985.

Gorse, C., Capitelli, M., and Ricard, A.: On the coupling of electron and vibrational energy distributions in H_2, N_2, and CO post discharges, J. Chem. Phys., 82(4), 1900–1906, 1985.

Harris, R. D. and Adams, G. W.: Where does the O(1D) energy go?, J. Geophys. Res., 88(A6), 4918–4928, 1983.

Hirao, K. and Oyama, K.: An improved type of electron temperature probe, J. Geomag. Geoelectr., 22, 393–402, 1970.

Hirao, K. and Oyama, K.-I.: Measurement of the space potential in plasma, J. Geomag. Geoelectr., 23, 47–60, 1971.

Hirao, K. and Oyama, K.: Comparison of cleaned and uncleaned probes on board a rocket, Space Res., XIII, 489–492, 1973.

Kummler, R. H. and Bortner, M. H.: Vibrational temperature in the E and F regions, Space Res., XII, 711–719, 1972.

Kurihara, J. and Oyama, K.-I.: Rocket instrument for measuring vibrational-rotational temperature and density in the lower thermosphere, Rev. Sci. Instr., 76, 083101, doi:10.1063/1.1988189, 2005.

Oyama, K.: A systematic investigation of several phenomena associated with contaminated Langmuir probes, Planet. Space Sci., 24, 183–190, 1976.

Oyama, K. and Hirao, K.: Application of grass-sealed Langmuir probe to ionosphere study, Rev. Sci. Instr., 47, 101–107, 1976.

Oyama, K. and Hirao, K.: Distortion of the energy distribution of ionospheric thermal electrons near the focus of Sq current vortex, Planet. Space Sci., 27, 183–192, 1979.

Oyama, K.-I. and Hirao, K.: Energy distribution of thermal electrons at the height of lower E region, Adv. Space. Res., 2(10), 89–91, 1983.

Oyama, K.-I. and Hirao, K.: Energy gain of thermal electrons from the excited neutral gases, J. Geomag. Geoelectr., 37, 913–926, 1985.

Oyama, K.-I., Hirao, K., Banks, P. M., and Williamson, P. R.: Is Te equal to Tn at the height of 100 to 120 km?, Planet. Space Sci., 28, 207–211, 1980.

Oyama, K.-I., Suzuki, K., Kawashima, N., Zalpuri, K. S., Tei, S., and Nakamura, Y.: An extreme ultraviolet radiation source for the simulation of the ionosphere, Rev. Sci. Instr., 62, 1721–1726, 1991.

Oyama, K.-I., Abe, T., Mori, H., and Liu, J. Y.: Electron temperature in nighttime sporadic E layer at mid-latitude, Ann. Geophys., 26, 533–541, doi:10.5194/angeo-26-533-2008, 2008.

Paniccia, F., Gorse, C., Bretagne, J., and Capitelli, M.: Electron energy distribution functions in molecular nitrogen, The role of super elastic electronic collisions in discharge and postdischarge conditions, J. Appl. Plys., 59, 4004–4006, 1986.

Pavlov, A. V.: The role of vibrationally excited oxygen and nitrogen in the D and E regions of the ionosphere, Ann. Geophys., 12, 1085–1090, doi:10.1007/s00585-994-1085-1, 1994.

Rohde, V., Piel, A., Thiemann, H., and Oyama, K.-I.: In situ diagnostics of ionospheric plasma with the resonance cone technique, J. Geophys. Res., 98, 19163–19172, 1993.

Schlapp, D. M.: Some measurements of collision frequency in the E region of the ionosphere, J. Atmos. Terr. Phys., 16, 340–343, 1959.

Schutz, Z. G. J.: Vibrational excitation N_2, CO, and H_2 by electron impact, Phys. Rev., 135(4A), A988–A994, 1964.

Shimoyama, M., Oyama, K.-I., and Abe, T.: Suprathermal Plasma Analyzer for the measurement of low-energy electron distribution in the ionosphere, in preparation, 2011.

Slanger, T. G. and Black, G.: Electronic-to-vibrational energy transfer efficiency in the $O(^1D)$- N_2 and $O(^1D)$- CO systems, J. Chem. Phys., 60, 468–477, 1974.

Smith, D.: The application of Langmuir probes to the measurement of very low electron temperatures, Planet. Space Sci., 20, 1717–1726, 1972.

Smith, L. G., Weeks, L. H., and Mckinnon, P. J.: Rocket observations of electron temperature in the E region, J. Atmos. Terr. Phys., 30, 1301–1312, 1968.

Spencer, N. W., Brace, L. H., and Carignan, G. R.: Electron temperature evidence for nonthermal equilibrium in the ionosphere, J. Geophys. Res., 67, 157–175, 1962.

Spencer, N. W., Brace, L. H., Carignan, G. R., Taeusch, D. R., and Niemann, H.: Electron and molecular nitrogen temperature and density in the thermosphere, J. Geophys. Res., 70, 2665–2698, 1965.

Sturges, D. J.: An evaluation of ionospheric probe performance – I. Evidence of contamination and clean-up of probe surfaces, Planet. Space. Sci., 21, 1029–1047, 1973.

Thrane, E. V. and Piggot, W. R.: The collision frequency in the E region and D regions of the ionosphere, J. Atmos. Terr. Phys., 28, 721–737, 1966.

Tonks, L. and Langmuir, I.: A general theory of the plasma of an arc, Phys. Rev., 34, 876–922, 1929.

Torr, M. R. and Torr, D. G.: The role of metastable species in the thermosphere, Rev. Geophys. Space Phys., 20, 91–144, 1982.

Walker, J. C. G.: Electron and nitrogen vibrational temperature in the E region of ionosphere, Planet. Space Sci., 16, 321–327, 1968.

Zalpuri, K. S. and Oyama, K.-I.: Theoretical estimation of the vibrational temperatures of N_2 molecules in the ionosphere and in the laboratory simulated plasma, ISAS Report RN642, 1991.